



## Journal of Advanced Research in Fluid Mechanics and Thermal Sciences

Journal homepage:  
[https://semarakilmu.com.my/journals/index.php/fluid\\_mechanics\\_thermal\\_sciences/index](https://semarakilmu.com.my/journals/index.php/fluid_mechanics_thermal_sciences/index)  
ISSN: 2289-7879



# Influence of Radiative Magnetic Field on a Convective Flow of a Chemically Reactive Hybrid Nanofluid over a Vertical Plate

Rajakumari Rammoorthi<sup>1</sup>, Dhivya Mohanavel<sup>1,\*</sup>

<sup>1</sup> Division of Mathematics, School of Advanced Sciences, Vellore Institute of Technology, Chennai Campus, Chennai-600 127, Tamil Nadu, India

### ARTICLE INFO

#### Article history:

Received 20 November 2022

Received in revised form 18 March 2023

Accepted 26 March 2023

Available online 14 April 2023

#### Keywords:

Hybrid nanofluid; vertical plate;  
radiation; magnetic field; Laplace  
transform technique

### ABSTRACT

This study pitch into the three different types of hybrids nanofluids flow across a semi-infinite moving vertical plate exposed to the radiative magnetic field and are also implanted in a porous medium. The governing equations corresponding to the problem is a linear partial differential equation which are simplified by appropriate non-dimensional quantities and solved using Laplace transform technique. Exact general solutions for the dimensionless velocity and temperature, concentration fields as well as the accompanying skin friction, Nusselt number and Sherwood number are graphically derived. Increase in the parameters like permeability, Grashof number for heat and mass elevates the hybrid nanofluids velocity profile. When the magnetic parameter increases there is a retardation in the flow speed. Heat transfer rate slows down when the radiation increase. It reveals that Prandtl number lowers thermal boundary layer thickness. Intensification of chemical reaction lowering the concentration. Elevation of Schmidt number, accelerates the mass transfer. This study, also have a keen interest in determining which type of hybrid nanofluid provides the greatest enhancement in velocity and temperature.

## 1. Introduction

Enhancing heat transfer is a challenge for contemporary technical fields like electronics, heat exchangers, chemical and biological reactors. Nanofluids are often viewed as effective media for enhancing energy transmission while hybrid nanofluids allow for the incorporation of two or more nanoadditives, which dramatically improves the transport processes more significantly.

While discussing nanofluids, we also come across the term called “nanofluidics” to clarify that, nanofluids are a type of fluid that contain nanoparticles, whereas nanofluidics deals with the behaviour of fluids which are manipulated and controlled when contained within a nanometer-sized structures. Both nanofluidics and nanofluids can exhibit novel physical behaviours are usually not observed in larger structures, which make them potentially useful in many applications. Increased interest in studying nanofluidics and nanofluids has resulted due to its recent developments in

\* Corresponding author.

E-mail address: [dhivya.m@vit.ac.in](mailto:dhivya.m@vit.ac.in)

<https://doi.org/10.37934/arfmts.105.1.90106>

nanotechnology which are explained by Yuting Zuo [1], Ji-Huan He *et al.*, [2] and Leigen Liu *et al.*, [3].

Currently, the study primarily focuses on nanofluids. The name "nanofluids" was coined by Choi and Eastman [4] who added a little amount of nanoparticle to the base fluid and discovered that thermal enhancement occurs more frequently in nanofluids than in other fluids. This finding has intrigued other researchers to help them examine their working fluid. Metals, non-metals, and metalloids can all be found in nanoparticles. Due to their characteristics and new uses in fields including optics, catalysis, electronics, medicine and biotechnology, metal nanoparticles have received a great deal of attention in this subject. Since metals have better thermal performance than non-metals and metalloids, so nanoparticles in this study are regarded as metals like aluminium (*Al*), silver (*Ag*) and copper (*Cu*).

Nehad Ali Shah *et al.*, [5] investigated an intensifying temperature and constant concentration of an electrically conducting incompressible fluid in an unstable magnetohydrodynamic-free convection flow across an infinite vertical plate and he also analysed about [6] the predominant hydrothermal and mass transport phenomena brought on by the convective flows of a remarkable non-homogeneous micropolar mixture over an impermeable horizontal electromagnetic surface, which is convectively heated in the presence of a particular changing heat source. Shah *et al.*, [7] investigated the study using type I and type II hybrid models, the dynamics of hybrid nanofluids with an emphasis on the differences between the two. This research discusses the effects of simultaneous stretching and suction on hybrid nanofluid boundary layer flow. Constatin Fetecau *et al.*, [8] addressed the concept of Newtonian heating along with mass diffusion, and chemical reaction of a hydromagnetic free convection flow across a rotating infinite vertical plate completely. Kiran Sajjan *et al.*, [9] explored the presence of Fourier fluxes and Boussinesq quadratic thermal oscillations, the impacts of linear, non-linear and quadratic Rosseland approximations on the behaviour of three-dimensional flows with ternary hybrid nanoparticles of various shapes and densities and Dinesh Kumar *et al.*, [10] has done with hybrid nanofluids. Rusdi *et al.*, [11] investigated the nanofluid penetrable flow over an exponentially diminishing sheet with heat radiation and partial slip of silver (*Ag*) nanoparticles in water and kerosene. Prasad *et al.*, [12] studied the radially stretched Riga plate transfers mass and heat from an unsteady, electrically conducting and viscous nanofluid. Using similarity variables from controlling flow equations, optimum Homotopy analysis was used to solve differential equations and also, he examined [13] magnetohydrodynamics flow and heat transfer in a nanofluid across a thin elastic sheet with changing fluid parameters. Translating non-linear governing equations into dimensionless form with proper boundary conditions, OHAM is utilised to solve the resulting equations. Prasad *et al.*, [14] examined the axisymmetric mixed convective MHD flow of a Casson nanofluid over a stretched variable thickness rotating disc with a heat source/sink and velocity slip surface boundary condition also investigated the thermal buoyancy and viscous dissipation and the disk's margins have convective heat and zero nanoparticle mass flux. The Optimal Homotopy Analysis Method is used to solve highly nonlinear coupled ordinary differential equations that are formed via the Von Karman similarity transformation (OHAM) and he also investigated [15] the mixed convective Williamson nanofluid flow on a spinning disc with negligible mass flux. Vaidya *et al.*, [16] analysed the electro-osmosis in peristaltic blood flow of MHD Carreau material with slip and changing material properties.

Abbasi *et al.*, [17] analysed the peristalsis phenomena of a water-based nanomaterial with temperature-dependent viscosity and thermal conductivity and standard nanoparticles in peristaltic motion, including copper, iron-oxide, gold and silver. Khashi'ie *et al.*, [18] investigated the concept of Joule heating of a hybrid nanofluid flow on a moving plate with heat transfer subjected to

magnetohydrodynamics (MHD) and he also analysed the numerical solutions in hybrid nanofluid flow for various physical aspects and surfaces, such as moveable plates, cylinders and discs. Zainal *et al.*, [20] analysed the heat transfer and MHD flow of a hybrid nanofluid towards a permeable moving surface while taking into account the thermal radiation effect. The authors demonstrate that there are dual solutions for both aiding and opposing flow within a given range of the movement parameters. Only one of the solutions is physically significant, according to a stability analysis. Aladdin *et al.*, [21] seeks to identify the presence of suction over a moving plate in a magnetic field environment. Khashi'ie *et al.*, [22] contributes their research focuses on the effect of a hybrid nanofluid on a moving solid surface with melting heat transfer. Rosca *et al.*, [23] discussed the problem of laminar axisymmetric flow of a hybrid nanofluid across a non-linearly stretching/shrinking permeable sheet with radiation influence, reported theoretical and numerical findings. Waini *et al.*, [24] investigated the flow towards a stretching/shrinking cylinder near the stagnation point of a hybrid nanofluid. Farooq *et al.*, [25] discussed the entropy formation of a hybrid nanofluid in the boundary layer flow across a nonlinear radially expanding porous disc in relation to suction/injection and viscous dissipation.

Muthucumaraswamy and Kulandaivel [26] discussed the presence of uniform heat flux and variable mass diffusion of the flow, across an infinite vertical plate spontaneously. Muthucumaraswamy and Ganesan [27] studied the effects of thermal radiation under variable temperature and mass diffusion on a moving infinite vertical plate. Loganathan and Dhivya [28] numerically studied the flow of an incompressible viscous fluid along an impulsively semi-infinite vertical cylinder immersed in a porous material and also, they enquired [29] about the moving, semi-infinite vertical cylinder contained in a porous media is subjected to the flow of a viscous, incompressible, energy-dissipating, electrically conducting, optically thin, and chemically reactive fluid in an unstable laminar free convective flow. Subhashini and Sumathi [30] used dual solutions to study the evolution of a mixed convection flow of nanofluids across a moving vertical plate. Loganathan and Deepa [31] studied about the casson fluid flow over a vertical permeable rigid plate.

Based on the literature, no investigation has been done to determine the impact of hybrid nanofluids in a moving vertical plate subjected to a radiative magnetic field embedded in a porous media. Utilizing the Laplace-transform method, the dimensionless governing equations are resolved. By varying the physical parameters and examining each hybrid nanofluid's velocity, heat, and mass transfer rates, it is possible to compare the performance of various hybrid nanofluids to determine which one has the best enhancement in its combination.

## 2. Mathematical Analysis

This article illustrates the incompressible flow of chemically reactive water base hybrid nanofluids in a radiative magnetic field embedded in a porous medium. The relevant physical model is illustrated in Figure 1. The three different nanoparticles, Aluminium (*Al*), Copper (*Cu*) and Silver (*Ag*) are combined to form three different hybrid nanofluids: *Al + Cu / water*, *Al + Ag / water* and *Cu + Ag / water*. The references for these hybrid nanofluids are given in [32-38]. This is done in order to demonstrate the thermal performance of these hybrid nanofluids. After some time, when  $t' > 0$ , the vertical plate moves with a constant velocity,  $u_0$  which is initially at rest. Using boundary layer approximation, a two-dimensional boundary layer governs the natural convective flow of incompressible viscous chemically reactive hybrid nanofluids over a semi-infinite vertical plate. Based on the literature [5,8] the governing equations for the current study considered as follows

$$\frac{\partial u}{\partial t'} = \frac{1}{\rho_{hnf}} \left( g(\beta\rho)_{hnf}(T' - T'_\infty) + g(\beta^*\rho)_{hnf}(C' - C'_\infty) + \mu_{hnf} \frac{\partial^2 u}{\partial y^2} - \sigma_{hnf} B_0^2 u - \mu_{hnf} \frac{u}{\lambda^*} \right) \quad (1)$$

$$\frac{\partial T'}{\partial t'} = \frac{1}{(\rho C_p)_{hnf}} \left( K_{hnf} \frac{\partial^2 T'}{\partial y^2} - \frac{\partial q_r}{\partial y} \right) \quad (2)$$

$$\frac{\partial C'}{\partial t'} = D \frac{\partial^2 C'}{\partial y^2} - k_r (C' - C'_\infty) \quad (3)$$

The physical initial conditions and boundary conditions to be satisfied

$$t' \leq 0; u = 0; T' = T'_\infty; C' = C'_\infty \text{ for all } y$$

$$t' > 0; u = u_0; T' = T'_w; C' = C'_w \text{ at } y = 0$$

$$u \rightarrow 0; T' \rightarrow T'_\infty; C' \rightarrow C'_\infty \text{ at } y \rightarrow \infty \quad (4)$$

where,  $u$  is the velocity in the directions of  $x$  - axis,  $t'$  is the time,  $T'_\infty$ ,  $T'_w$ ,  $C'_w$  and  $C'_\infty$  as free stream temperature, wall temperature, free stream concentration and wall concentration,  $D$  is the mass diffusivity,  $g$  is the acceleration due to gravity, is the radioactive heat flux,  $C_p$  is the specific heat capacity,  $\beta$  is the thermal expansion's volumetric coefficient,  $\beta^*$  a concentration's volumetric coefficient of expansion,  $B_0$  is dimensional magnetic parameter,  $\lambda^*$  is the permeability medium, and  $k_r$  is the chemical reaction parameter. To show unidirectional radiative heat flux, we utilize the Rosseland estimation which gives the accompanying radiative heat flux as

$$q_r = \frac{-4\sigma^* \partial T'^4}{3K^* \partial y} \quad (5)$$

where  $\sigma^*$  denotes the Stefan-Boltzmann constant and  $k^*$  denotes the mean absorption coefficient. For the situation of an optically thin grey gas, the local radiant is expressed where  $a^*$  is the absorption coefficient.

$$\frac{\partial q_r}{\partial x} = -4 a^* \sigma^* (T_\infty^4 - T^4) \quad (6)$$

In order to extend the Taylor series  $T^4$  about  $T_\infty$  and disregard the second and higher order components, assuming a minimal difference between the fluid's temperature  $T$  and the temperature of the free stream  $T_\infty$ .

$$T^4 \cong 4T'^3 T' - 3T_\infty'^4 \quad (7)$$

Here  $\rho_{hnf}$ ,  $(\rho C_p)_{hnf}$ ,  $\mu_{hnf}$  and  $K_{hnf}$  are density, heat capacitance, dynamic viscosity and thermal conductivity of hybrid nanofluids then subscripts  $f, s_1, s_2$  represents the basefluid, nanoparticle 1 and nanoparticle 2. The water-based hybrid nanofluid including distinguished nanoparticles combinations of  $Al$ ,  $Ag$  and  $Cu$ , the thermophysical properties of these are presented in Table 1. Table 2 represent the properties of hybrid nanofluid which is computed from the given formula using the thermo-physical characteristics of base fluid and nanoparticles.

**Table 1**  
 Thermo-physical characteristics of nanoparticles and water [17]

Thermo-physical characteristics	Nanoparticles			
	$H_2O$	$Al$	$Cu$	$Ag$
$\rho$ ( $kg/m^3$ )	997.1	2700	8933	10500
$C_p$ ( $J/kg^1K^1$ )	4179	903	385	235
$K$ ( $W/m^1k^1$ )	0.613	236	401	429
$\beta$ ( $1/k$ ) $\times 10^{-6}$	210	23	16.7	18.9
$\beta^*$ ( $1/k$ ) $\times 10^{-6}$	214	69	50.1	56.7

**Table 2**  
 Hybrid nanofluids correlation [18]

Properties	Hybrid nanofluids
Density ( $\rho$ )	$\rho_{hnf} = (1 - \phi_{hnf})\rho_f + \phi_1 \rho_{s_1} + \phi_2 \rho_{s_2}$
Heat Capacity ( $\rho C_p$ )	$(\rho C_p)_{hnf} = (1 - \phi_{hnf})(\rho C_p)_f + \phi_1 (\rho C_p)_{s_1} + \phi_2 (\rho C_p)_{s_2}$
Dynamic Viscosity ( $\mu$ )	$\frac{\mu_{hnf}}{\mu_f} = \frac{1}{(1 - \phi_{hnf})^{2.5}}$
Thermal conductivity ( $K$ )	$\frac{K_{hnf}}{K_f} = \frac{\left(\frac{\phi_1 K_1 + \phi_2 K_2}{\phi_{hnf}}\right) + 2 K_f + 2(\phi_1 K_1 + \phi_2 K_2) - 2\phi_{hnf} K_f}{\left(\frac{\phi_1 K_1 + \phi_2 K_2}{\phi_{hnf}}\right) + 2 K_f - (\phi_1 K_1 + \phi_2 K_2) - \phi_{hnf} K_f}$

The three major equations mass, momentum and energy are the three governing equations for natural convection flow, which are linear partial differential equations. The necessary non-dimensional quantities for the governing Eq. (1), Eq. (2) and Eq. (3) are introduced.

$$U = \frac{u}{u_0}; \quad Y = \frac{yu_0}{v_f}; \quad t = \frac{t'u_0}{v_f}; \quad \theta = \frac{(T' - T'_\infty)}{(T'_w - T'_\infty)}; \quad C = \frac{(C' - C'_\infty)}{(C'_w - C'_\infty)}$$

$$Gr = \frac{g\beta(T'_w - T'_\infty)v_f}{u_0^3}; \quad Gm = \frac{g\beta^*(C'_w - C'_\infty)v_f}{u_0^3}; \quad M = \frac{\sigma_{hnf}B_0^2v_f}{\rho_f u_0^2}$$

Using the non-dimensional quantities mentioned above and the Rosseland approximation Eq. (5), equations Eq. (1), Eq. (2) and Eq. (3) are simplified. The simplified equations in the form of Eq. (8), Eq. (9) and Eq. (10).

$$\frac{\partial U}{\partial t} = \alpha_1 Gr\theta + \alpha_2 GmC + \alpha_3 \frac{\partial^2 U}{\partial Y^2} - \alpha \tag{8}$$

$$\frac{\partial \theta}{\partial t} = (\alpha_5 + \alpha_6) \frac{\partial^2 \theta}{\partial y^2} \tag{9}$$

$$\frac{\partial C}{\partial t} = \frac{1}{Sc_f} \frac{\partial^2 C}{\partial y^2} - Kc_f \tag{10}$$

where

$$\alpha = \alpha_4 M + \frac{\alpha_5}{\lambda}$$

$$\alpha_1 = \frac{(1 - \phi_{hnf}) + \phi_1 \frac{(\beta\rho)_{s_1}}{(\beta\rho)_f} + \phi_2 \frac{(\beta\rho)_{s_2}}{(\beta\rho)_f}}{(1 - \phi_{hnf}) + \phi_1 \frac{\rho_{s_1}}{\rho_f} + \phi_2 \frac{\rho_{s_2}}{\rho_f}}$$

$$\alpha_2 = \frac{(1 - \phi_{hnf}) + \phi_1 \frac{(\beta^*\rho)_{s_1}}{(\beta^*\rho)_f} + \phi_2 \frac{(\beta^*\rho)_{s_2}}{(\beta^*\rho)_f}}{(1 - \phi_{hnf}) + \phi_1 \frac{\rho_{s_1}}{\rho_f} + \phi_2 \frac{\rho_{s_2}}{\rho_f}}$$

$$\alpha_3 = \frac{1}{(1 - \phi_{hnf})^{2.5} \left\{ (1 - \phi_{hnf}) + \phi_1 \frac{\rho_{s_1}}{\rho_f} + \phi_2 \frac{\rho_{s_2}}{\rho_f} \right\}}$$

$$\alpha_4 = \frac{1}{(1 - \phi_{hnf}) + \phi_1 \frac{\rho_{s_1}}{\rho_f} + \phi_2 \frac{\rho_{s_2}}{\rho_f}}$$

$$\alpha_5 = \frac{K_{hnf}}{Pr_f K_f} \frac{1}{(1 - \phi_{hnf}) + \phi_1 \frac{(\rho C_p)_{s_1}}{(\rho C_p)_f} + \phi_2 \frac{(\rho C_p)_{s_2}}{(\rho C_p)_f}}$$

$$\alpha_6 = \frac{16\sigma^* T_\infty^3}{3k^*} \frac{1}{Pr_f K_f} \frac{1}{(1 - \phi_{hnf}) + \phi_1 \frac{(\rho C_p)_{s_1}}{(\rho C_p)_f} + \phi_2 \frac{(\rho C_p)_{s_2}}{(\rho C_p)_f}}$$

For the following non-dimensional Eq. (4), the appropriate initial conditions and boundary conditions are expressed as an Eq. (11)

$$\begin{aligned} t' \leq 0; U = 0; \theta = 0; C = 0 \text{ for all } Y \\ t' > 0; U = 1; \theta = 1; C = 1 \text{ at } Y = 0 \\ U \rightarrow 0; \theta \rightarrow \infty; C \rightarrow \infty \text{ at } Y \rightarrow \infty \end{aligned} \tag{11}$$

where  $U$  is the dimensionless velocity in the axial  $X$  – coordinate,  $\theta$  is the dimensionless temperature,  $C$  is the dimensionless concentration,  $Gr$  and  $Gm$  are Grashof number for heat and mass transfer  $Pr$ ,  $Sc$ ,  $Kc_f$ ,  $M$  and  $\lambda$  which represent the parameters Prandtl number, Schmidt number, chemical reaction, magnetic and permeability.

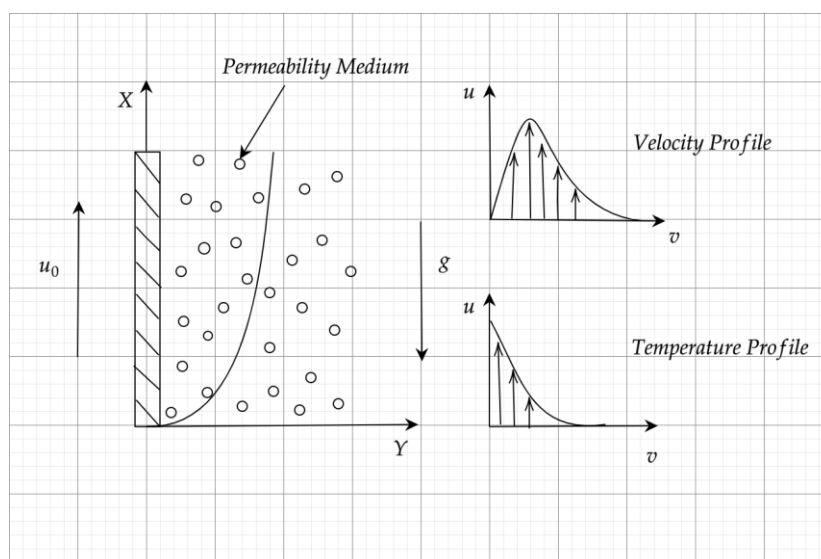


Fig. 1. Physical model of the problem

### 3. Analytical Solution

Many researchers in applied science, mathematics, engineering and benevolent calibration of integral differential, circuit systems and mechanical systems employ the Laplace transform. The Laplace transform is used to solve linear differential equations of second or higher order. The Laplace transform, its characteristics and its numerous applications were discussed by Bhullar and Malkeet [19]. A typical Laplace transform approach has been used to extract velocity  $U$ , temperature  $T$  and

concentration  $C$  in order to resolve the unstable, dimensionless overseeing conditions Eq. (8) to Eq. (10) under the boundary conditions Eq. (11). Using the formula,

$$L^{-1}\left(\frac{e^{-Y\sqrt{p+b}}}{p-a}\right) = e^{-Y\sqrt{a+b}} \operatorname{erfc}\left(\frac{Y}{2\sqrt{t}} - \sqrt{(a+b)t}\right) + e^{Y\sqrt{a+b}} \operatorname{erfc}\left(\frac{Y}{2\sqrt{t}} + \sqrt{(a+b)t}\right)$$

$$\operatorname{erfc}(x) = 1 - \operatorname{erf}(x) = \frac{2}{\sqrt{\pi}} \int_x^{\infty} e^{-t^2} dt$$

Let us consider

$$N_1 = \frac{\alpha_1 \alpha_3 (\alpha_5 + \alpha_6)}{\alpha_3 - \alpha_5 - \alpha_6} \quad N_2 = \frac{\alpha_7 (\alpha_5 + \alpha_6)}{\alpha_3 - \alpha_5 - \alpha_6}$$

$$N_3 = \frac{\alpha_1 \alpha_3}{Sc_f \alpha_3 - 1} \quad N_4 = \frac{Sc_f k_{cf} \alpha_3 - \alpha}{Sc_f \alpha_3 - 1}$$

$$U = \left(\frac{1}{2} + \frac{N_1 Gr}{2 N_2} - \frac{N_3 Gm}{2 N_4}\right) \left( e^{-\sqrt{\frac{\alpha}{\alpha_3}} Y} \operatorname{erfc}\left(\frac{Y}{2\sqrt{\alpha_3 t}} - \sqrt{\alpha t}\right) + e^{\sqrt{\frac{\alpha}{\alpha_3}} Y} \operatorname{erfc}\left(\frac{Y}{2\sqrt{\alpha_3 t}} + \sqrt{\alpha t}\right) \right)$$

$$- \left(\frac{N_1 Gr e^{N_2 t}}{2 N_2}\right) \left( e^{-\sqrt{\frac{\alpha + N_2}{\alpha_3}} Y} \operatorname{erfc}\left(\frac{Y}{2\sqrt{\alpha_3 t}} - \sqrt{(\alpha + N_2)t}\right) + e^{\sqrt{\frac{\alpha + N_2}{\alpha_3}} Y} \operatorname{erfc}\left(\frac{Y}{2\sqrt{\alpha_3 t}} + \sqrt{(\alpha + N_2)t}\right) \right)$$

$$+ \left(\frac{N_3 Gm e^{-N_4 t}}{2 N_4}\right) \left( e^{-\sqrt{\frac{\alpha - N_4}{\alpha_3}} Y} \operatorname{erfc}\left(\frac{Y}{2\sqrt{\alpha_3 t}} - \sqrt{(\alpha - N_4)t}\right) + e^{\sqrt{\frac{\alpha - N_4}{\alpha_3}} Y} \operatorname{erfc}\left(\frac{Y}{2\sqrt{\alpha_3 t}} + \sqrt{(\alpha - N_4)t}\right) \right)$$

$$- \left(\frac{N_1 Gr}{N_2}\right) \operatorname{erfc}\left(\frac{Y}{2\sqrt{(\alpha_5 + \alpha_6)t}}\right)$$

$$- \left(\frac{N_1 Gr e^{N_2 t}}{2 N_2}\right) \left( e^{-\sqrt{\frac{N_2}{(\alpha_5 + \alpha_6)}} Y} \operatorname{erfc}\left(\frac{Y}{2\sqrt{(\alpha_5 + \alpha_6)t}} - \sqrt{N_2 t}\right) + e^{\sqrt{\frac{N_2}{(\alpha_5 + \alpha_6)}} Y} \operatorname{erfc}\left(\frac{Y}{2\sqrt{(\alpha_5 + \alpha_6)t}} + \sqrt{N_2 t}\right) \right)$$

$$+ \left(\frac{N_3 Gm}{2 N_4}\right) \left( e^{-\sqrt{K_{cf} Sc_f} Y} \operatorname{erfc}\left(\frac{Y\sqrt{Sc_f}}{2\sqrt{t}} - \sqrt{K_{cf} t}\right) + e^{\sqrt{K_{cf} Sc_f} Y} \operatorname{erfc}\left(\frac{Y}{2\sqrt{t}} + \sqrt{K_{cf} t}\right) \right)$$

$$+ \left(\frac{N_3 Gm e^{-N_4 t}}{2 N_4}\right) \left( e^{-\sqrt{(K_{cf} - N_4) Sc_f} Y} \operatorname{erfc}\left(\frac{Y\sqrt{Sc_f}}{2\sqrt{t}} - \sqrt{(K_{cf} - N_4)t}\right) + e^{\sqrt{(K_{cf} - N_4) Sc_f} Y} \operatorname{erfc}\left(\frac{Y\sqrt{Sc_f}}{2\sqrt{t}} + \sqrt{(K_{cf} - N_4)t}\right) \right)$$
(12)

$$C = \frac{1}{2} e^{-\sqrt{K_{cf} Sc_f} Y} \operatorname{erfc}\left(\frac{Y\sqrt{Sc_f}}{2\sqrt{t}} - \sqrt{K_{cf} t}\right) + \frac{1}{2} e^{\sqrt{K_{cf} Sc_f} Y} \operatorname{erfc}\left(\frac{Y}{2\sqrt{t}} + \sqrt{K_{cf} t}\right)$$
(13)

$$\theta = \operatorname{erfc}\left(\frac{Y}{2\sqrt{(\alpha_5 + \alpha_6)t}}\right)$$
(14)

The expressions for Nusselt and Sherwood numbers are given by

$$Nu = -\left.\frac{\partial T}{\partial Y}\right|_{Y=0} = \frac{1}{t\sqrt{\pi}\sqrt{e+f}}$$
(15)

$$Sh = -\frac{\partial C}{\partial Y}\Big|_{Y=0} = \frac{e^{-K_c t}}{\sqrt{\pi} \sqrt{Sc}} - \frac{1}{2} \operatorname{erfc} \left( \sqrt{K_c t} \right) \sqrt{K_c Sc} \frac{1}{2} - \frac{1}{2} \left( \operatorname{erfc} \left( \sqrt{K_c t} \right) - 2 \right) \sqrt{K_c Sc} \quad (16)$$

The skin friction coefficient is given by

$$C_f = -\frac{\partial U}{\partial Y}\Big|_{Y=0} \quad (17)$$

#### 4. Results and Discussions

The flow behaviour depicted by Eq. (12)-(14), are based on the values obtained through MATLAB programming. Figure 2 demonstrates the effect of permeability parameter in velocity profile. It has been observed that the velocity and thickness of the boundary layer emerge with large values of  $\lambda$ . The boundary layer thickness determines how far the flow has travelled from its surface boundary to the point at which it has attained free-stream velocity. The porous medium construction enhances velocity distribution at higher permeability parameters. Larger pores in the porous media cause bulk fluid motion, which boosts velocity. We may infer that *Al + Cu / water* has superior enhancement. The hybrid nanofluid *Cu + Ag / water* retards the fluid flow than any other hybrid nanofluids.

An appropriate magnetic field can be used to influence the boundary layer behaviour. By varying the structure of the boundary layer, the MHD principle may be used to regulate the flow field in the desired direction. The magnetic parameter ( $M$ ) determines the strength of the applied magnetic field. The physical magnitude of the applied magnetic field and the electrical conductivity are dependent on the magnetic parameter. If the magnetic field is taken in the direction opposite to that of the flow field, then the magnetic parameter ( $M$ ) is considered to be negative which elevates the velocity of the flow. It is in proportion to density and viscosity of the fluid. Figure 3 depicts the magnetic impact on the velocity profile of three separate hybrid nanofluids. When the magnetic parameter is negative, the velocity distribution is substantial, and when it is positive, the distribution is minimal. *Cu + Ag / water* magnetic effect is slightly weaker than the other two. *Al + Cu / water* dominates *Al + Ag / water* that can be seen in Figure 3. Aluminium dominates in both situations. We may deduce that when the magnetic parameter is altered, *Al + Cu / water* performs better.

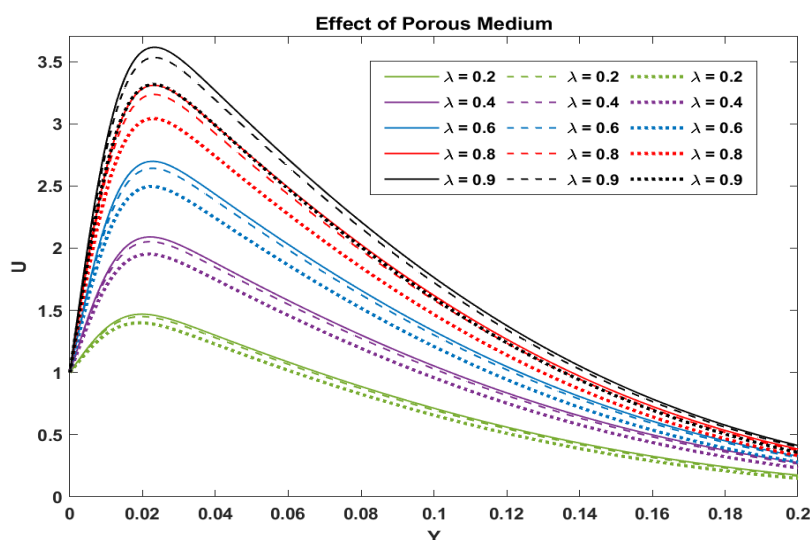


**Fig. 2.** (Solid lines – *Al + Cu / water*; Dashed lines – *Al + Ag / water*; Dotted lines – *Cu + Ag / water*)



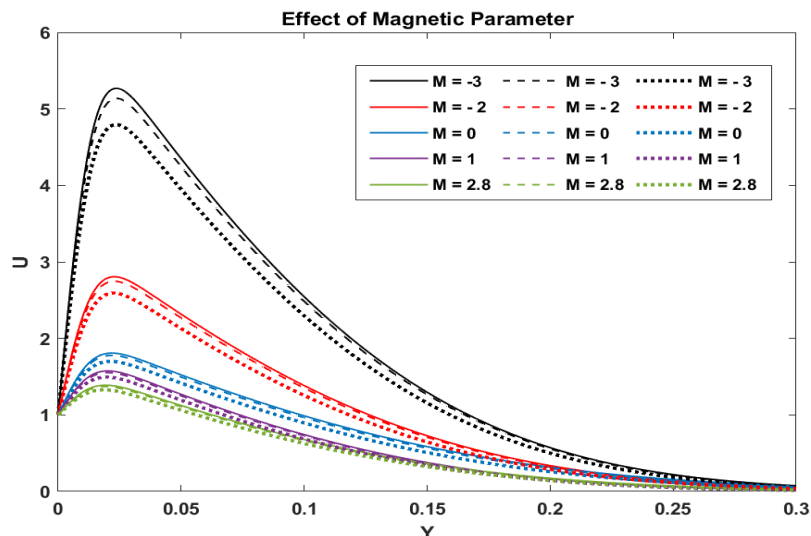


**Fig. 3.** (Solid lines – *Al + Cu / water*; Dashed lines – *Al + Ag / water*; Dotted lines – *Cu + Ag / water*)

Grashof number is described as the proportion of the buoyancy forces to the viscous forces that are present in the fluid. Since buoyancy forces are the driving forces behind the natural convection, this is essential for the current investigation. Natural convection caused by heat transfer at a solid surface submerged in a liquid  $Gr$  and  $Gm$ , is a non-dimensional quantity used in the analysis of heat and mass transfer. Figure 4 illustrates the effect  $Gr$  on the flow distribution in a velocity profile. An increase in  $Gr$  indicates an increase in temperature gradients, which in turn increases in the velocity distribution. Figure 5 depicts the effect of the  $Gm$ , the velocity profile is observed to be improved by the increase in  $Gm$ . It is clearly seen that the *Al + Cu / water* has an elevated in  $Gr$  and  $Gm$ . Figure 6 demonstrating the three different hybrid nanofluids velocity profile with pertinent parameters. By demonstrating all of the physical parameters like permeability, magnetic parameter, Grashof number for heat and mass and deciphering the graph, we analysed that aluminium and copper dominates in all the parameters. We are able to make the prediction that the velocity profile of *Al + Cu / water* is superior than other hybrid nanofluids.

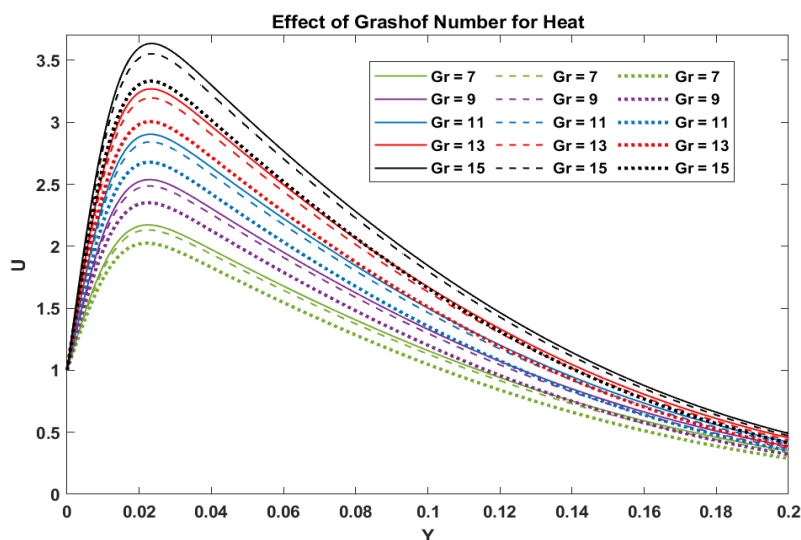


**Fig. 4.** (Solid lines – *Al + Cu / water*; Dashed lines – *Al + Ag / water*; Dotted lines – *Cu + Ag / water*)

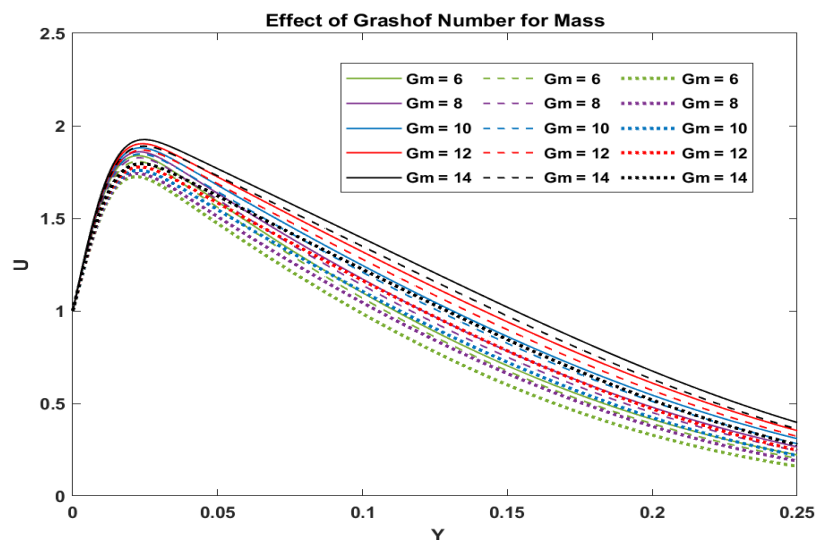


**Fig. 5.** (Solid lines – *Al + Cu / water*; Dashed lines – *Al + Ag / water*; Dotted lines – *Cu + Ag / water*)

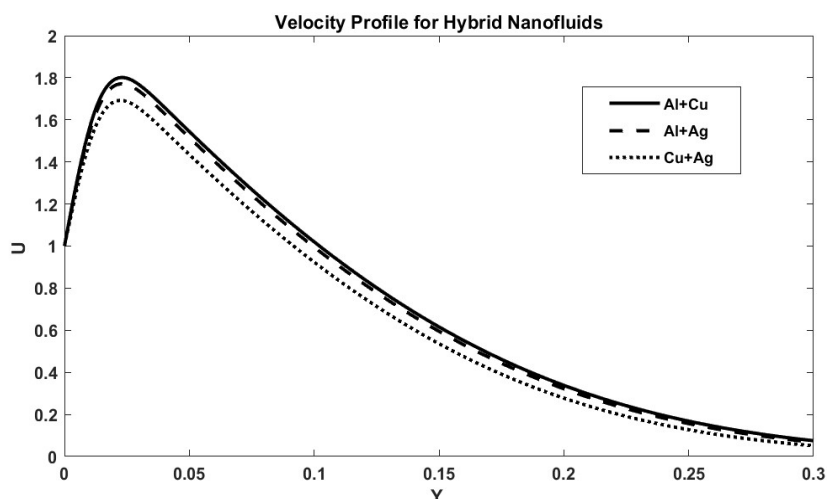


**Fig. 6.** Velocity profile for hybrid nanofluid ( $t = 0.01, N = 2, Pr = 6.2, Sc = 0.6, kc = 6, M = 0, \lambda = 0, Gr = 5, Gm = 3$ )

Investigated the concentration of hybrid nanofluids where all the three hybrid nanofluids behaves the same because the Eq. (13) do not contain physical properties such as density, specific heat capacity, thermal conduction and viscosity. Figure 7 illustrates the effect of chemical reaction parameter in the concentration profile. When the rate of chemical reaction increases, the particle breaks and the liquid gets diluted which weakens the concentration. Figure 8 demonstrates the effect of Schmidt number, increase in the Schmidt number increases the concentration of the hybrid nanofluids this is due to the increase in mass diffusion rate in the concentration term. Figure 9 exhibits mass transfer rate for different Schmidt numbers. Regardless of fluid, higher  $Sc$  values increase mass transfer rate related with concentration gradient.

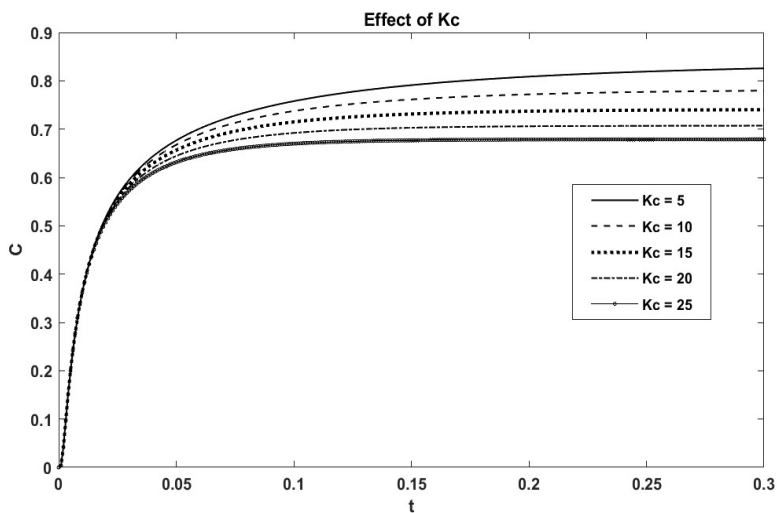


**Fig. 7.** The effect of chemical reaction parameter in the concentration profile

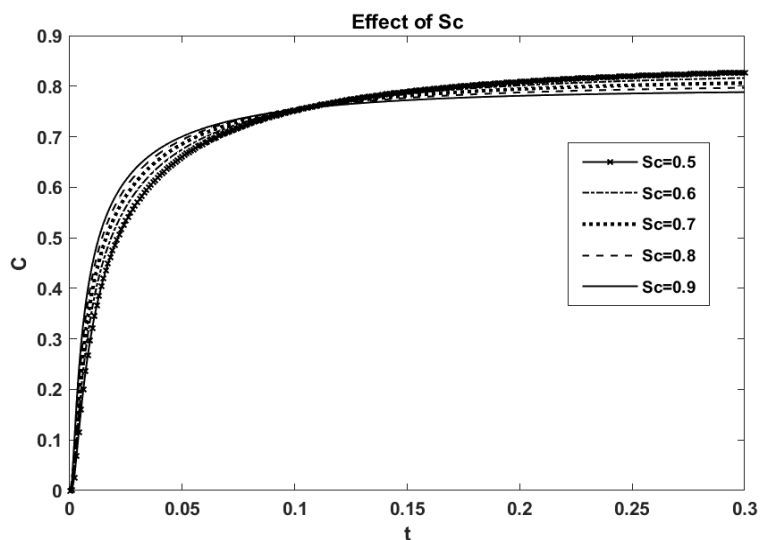


**Fig. 8.** The effect of Schmidt number, increase in the Schmidt number increases the concentration of the hybrid nanofluids this is due to the increase in mass diffusion rate in the concentration term

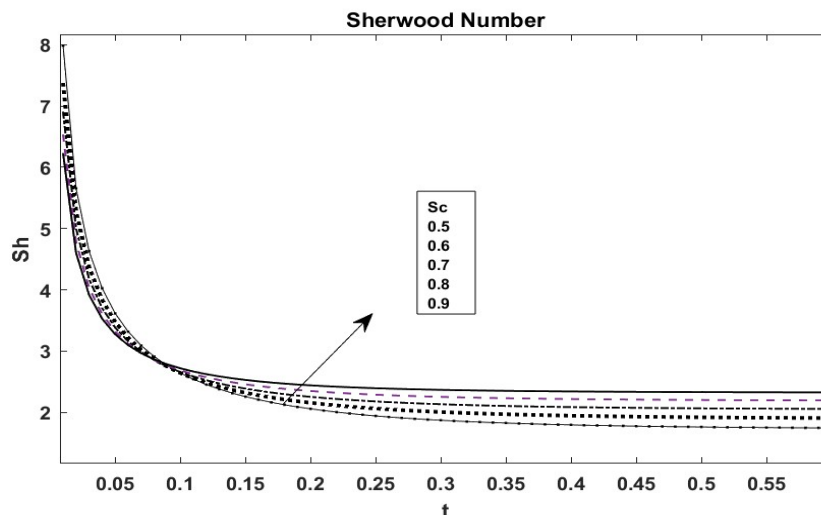


Fig. 9. Mass transfer rate for different Schmidt numbers

Figure 10 illustrates the effect of Prandtl number. As  $Pr$  increases, thermal diffusivity decreases, results a thinner thermal boundary layer. The region of fluid flow characterised by a temperature gradient is referred as thermal boundary layer. The distance from the surface to the point where the temperature of the flow is identical to the temperature of the free-stream determines the thickness of the thermal boundary layer. Figure 11 illustrates the effect of radiation parameter in the temperature profile. High-energy electrons decline in energy during radiation energy transit, which results in the temperature drop. In this study,  $Al + Ag / water$  has better enhancement comparing to other hybrid nanofluids. Figure 12 depicts the Nusselt number for various Prandtl number values. The permitted  $Pr$  parameter improves the transfer of energy from a high-temperature area to a low-temperature area. It can be seen from the graphs that  $Al + Ag / water$  has the better enhancement in temperature profile. This is due to the fact that silver has a higher thermal conductivity than copper and aluminium. The temperature profile of the hybrid nanofluids  $Al + Ag / water$  and  $Cu + Ag / water$  that contain silver nanoparticles has been improved, whereas  $Al + Cu / water$  does not have a better profile because of a lack of silver nanoparticles.

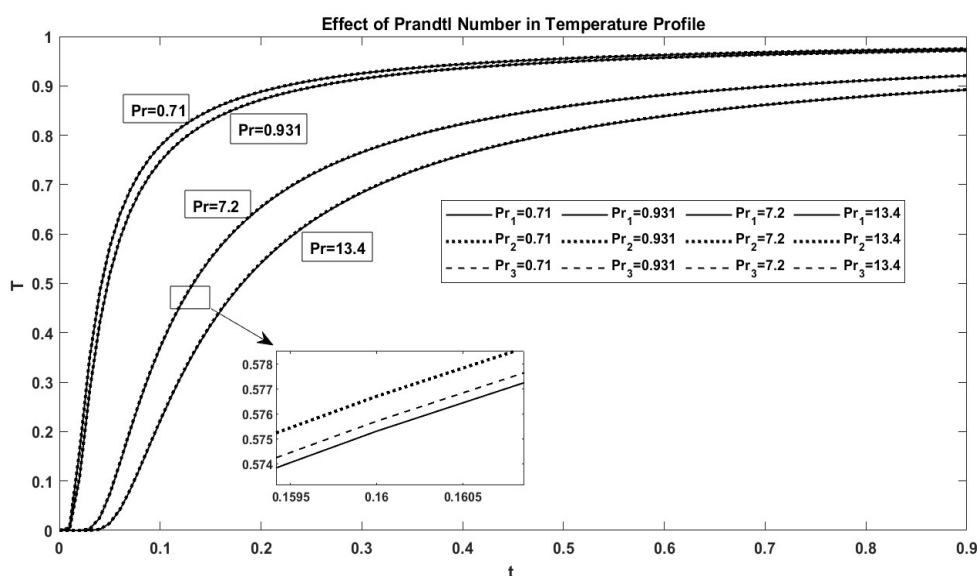
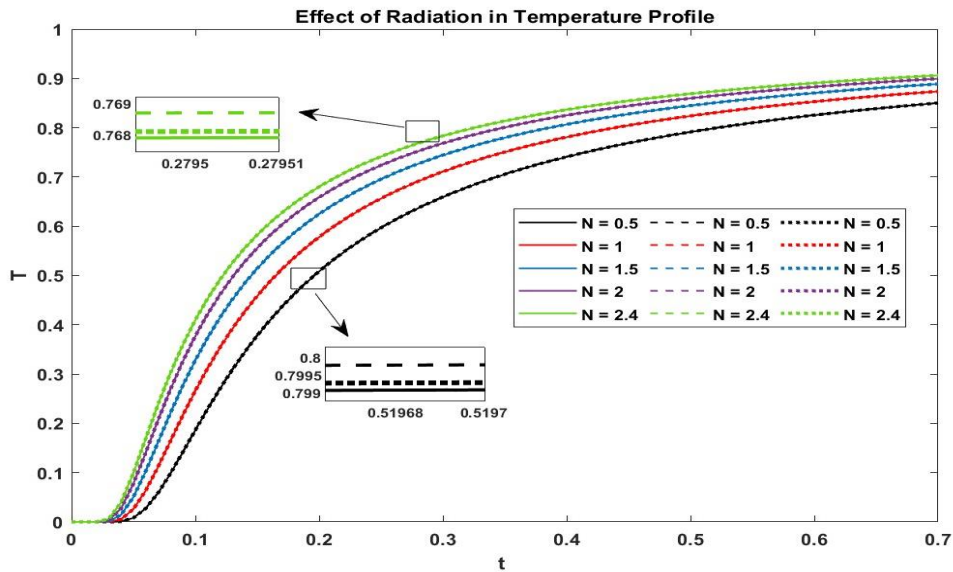
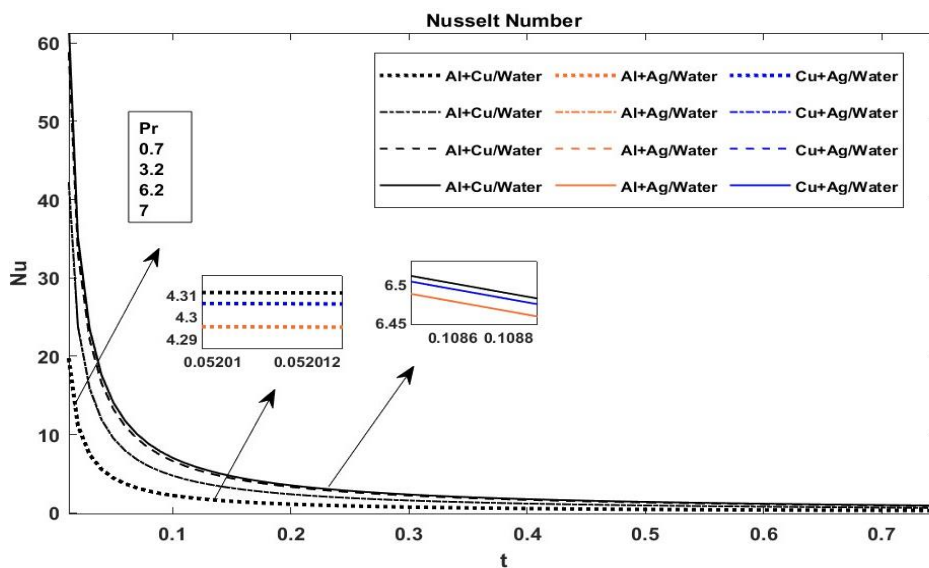


Fig. 10.  $Pr_1$  – Prandtl Number for  $Al + Cu / water$ ;  $Pr_2$  – Prandtl Number for  $Al + Ag / water$ ;  $Pr_3$  – Prandtl Number for  $Cu + Ag / water$



**Fig. 11.** (Solid lines – Al + Cu / water; Dashed lines – Al + Ag / water; Dotted lines – Cu + Ag / water)



**Fig. 12.** The Nusselt number for various Prandtl number values

Table 3 examines the viscous drag of the fluid flow. As the flow rate increases, the skin friction coefficient drops. When the permeability parameter increases, there is a decrease in the skin friction coefficient owing to the fact that fluid flow is elevated as permeability increases. It can be evidently seen that there is an increase in viscous drag as  $M$  increases.

**Table 3**

Skin friction coefficient for different values of  $N, M$ , and  $\lambda$  with  $Pr = 6.2, Sc = 0.6, kc = 6, Gr = 5, Gm = 3$  and  $t = 0.08$ ;

$C_{f_1}$  = Skin friction coefficient of  $Al + Cu / water$

$C_{f_2}$  = Skin friction coefficient of  $Al + Ag / water$

$C_{f_3}$  = Skin friction coefficient of  $Cu + Ag / water$

$\lambda$	$M$	$N$	$C_{f_1}$	$C_{f_2}$	$C_{f_3}$
0.2	1.8	2.0	0.44919	0.56515	0.82837
0.2	1.9	2.0	0.49713	0.61571	0.87534
0.3	2.0	0.5	-2.90953	-2.67998	-2.17127
0.3	2.0	1.0	-1.79930	-1.60587	-1.18075
0.3	2.0	1.1	-1.63377	-1.44574	-1.03312
0.3	1.0	1.2	-2.12822	-1.923106	-1.48813
0.3	1.5	1.2	-1.87758	-1.68132	-1.25499
0.3	2.0	1.5	-1.08649	-0.91633	-0.54508
0.3	1.8	2.0	-0.70933	-0.55144	-0.21037
0.3	1.9	2.0	-0.64425	-0.48853	-0.15157
0.4	1.8	2.0	-0.96312	-0.79564	-0.45497

## 5. Conclusions

The impact of convective flow of three different chemically reactive hybrid nanofluids in a porous material exposed to a radiative magnetic field has been examined in this research. Analytical solutions for the non-dimensional governing equations of momentum, energy and concentration are found using the Laplace transform. Graphical representations show the velocity, temperature and concentration profiles of different parameters of three hybrid nanofluids. Results include the following

- i. In Comparison with other hybrid nanofluids,  $Al + Cu / water$  has better performance and enhancement in the velocity profile. The profile of the velocity term is raised as the magnetic parameter shifts to the negative. When the values of  $M$  increase, the flow velocity of hybrid nanofluids considerably reduces throughout the fluid domain.
- ii. Increase in  $Gm$  and  $Gr$ , improves the velocity profile of hybrid nanofluids. It can be concluded that the permeability parameter causes the velocity profile of hybrid nanofluids to grow.
- iii. The radiation parameter can be changed to exhibit different temperature profiles. The proportion of conduction heat transfer to thermal radiation transfer is defined by the radiation parameter. Conduction heat transfer will rise as radiation does, improving temperature profiles. Increase in Prandtl number results in a downward shift in the temperature profile.  $Al + Ag / water$  has better performance and enhancement in the temperature profile.
- iv. The physical factors do not affect the hybrid nanofluids concentration term, it is the same. Schmidt number,  $Sc$  and chemical reaction,  $kc$  all have an effect on concentration term. The link between the rates of mass diffusion and viscosity is represented by the Schmidt number. When the Schmidt number rises, the rate of mass diffusion will likewise decrease, which will result in a rise in the and viscosity is represented by the Schmidt number; when the Schmidt number rises, the rate of mass diffusion will likewise decrease, which will result in a rise in the concentration profile. When the chemical reaction parameter  $kc$  is reduced, the concentration of the hybrid nanofluids increases.

## Acknowledgement

This research was not funded by any grant.

## References

- [1] Zuo, Yuting. "Effect of SiC particles on viscosity of 3-D print paste: A fractal rheological model and experimental verification." *Thermal Science* 25, no. 3 Part B (2021): 2405-2409. <https://doi.org/10.2298/TSCI200710131Z>
- [2] He, Ji-Huan, and Nader Y. Abd Elazem. "The carbon nanotube-embedded boundary layer theory for energy harvesting." *Facta Universitatis, Series: Mechanical Engineering* 20, no. 2 (2022): 211-235. <https://doi.org/10.22190/FUME220221011H>
- [3] Liu, Leigen, Yan-Qing Liu, Yun-Yu Li, Yue Shen, and Ji-Huan He. "Dropping in electrospinning process: a general strategy for fabrication of microspheres." *Thermal Science* 25, no. 2 Part B (2021): 1295-1303. <https://doi.org/10.2298/TSCI191228025L>
- [4] Choi, S. US, and Jeffrey A. Eastman. *Enhancing thermal conductivity of fluids with nanoparticles*. No. ANL/MSD/CP-84938; CONF-951135-29. Argonne National Lab.(ANL), Argonne, IL (United States), 1995.
- [5] Shah, Nehad Ali, Azhar Ali Zafar, and Shehraz Akhtar. "General solution for MHD-free convection flow over a vertical plate with ramped wall temperature and chemical reaction." *Arabian Journal of Mathematics* 7 (2018): 49-60. <https://doi.org/10.1007/s40065-017-0187-z>
- [6] Shah, Nehad Ali, Abderrahim Wakif, Essam R. El-Zahar, Sohail Ahmad, and Se-Jin Yook. "Numerical simulation of a thermally enhanced EMHD flow of a heterogeneous micropolar mixture comprising (60%)-ethylene glycol (EG),(40%)-water (W), and copper oxide nanomaterials (CuO)." *Case Studies in Thermal Engineering* 35 (2022): 102046. <https://doi.org/10.1016/j.csite.2022.102046>
- [7] Shah, Nehad Ali, I. L. Animasaun, Abderrahim Wakif, O. K. Koriko, R. Sivaraj, K. S. Adegbeie, Zahra Abdelmalek, H. Vaidyaa, A. F. Ijirimoye, and K. V. Prasad. "Significance of suction and dual stretching on the dynamics of various hybrid nanofluids: Comparative analysis between type I and type II models." *Physica Scripta* 95, no. 9 (2020): 095205. <https://doi.org/10.1088/1402-4896/aba8c6>
- [8] Fetecau, Constatin, Nehad Ali Shah, and Dumitru Vieru. "General solutions for hydromagnetic free convection flow over an infinite plate with Newtonian heating, mass diffusion and chemical reaction." *Communications in Theoretical Physics* 68, no. 6 (2017): 768. <https://doi.org/10.1088/0253-6102/68/6/768>
- [9] Sajjan, Kiran, Nehad Ali Shah, N. Ameer Ahammad, C. S. K. Raju, M. Dinesh Kumar, and Wajaree Weera. "Nonlinear Boussinesq and Rosseland approximations on 3D flow in an interruption of Ternary nanoparticles with various shapes of densities and conductivity properties." *AIMS Math* 7, no. 10 (2022): 18416-18449. <https://doi.org/10.3934/math.20221014>
- [10] Kumar, M. Dinesh, C. S. K. Raju, Kiran Sajjan, Essam R. El-Zahar, and Nehad Ali Shah. "Linear and quadratic convection on 3D flow with transpiration and hybrid nanoparticles." *International Communications in Heat and Mass Transfer* 134 (2022): 105995. <https://doi.org/10.1016/j.icheatmasstransfer.2022.105995>
- [11] Rusdi, Nadia Diana Mohd, Siti Suzilliana Putri Mohamed Isa, Norihan Md Arifin, and Norfifah Bachok. "Thermal Radiation in Nanofluid Penetrable Flow Bounded with Partial Slip Condition." *CFD Letters* 13, no. 8 (2021): 32-44. <https://doi.org/10.37934/cfdl.13.8.3244>
- [12] Prasad, K. V., C. Rajashekhar, F. Mebarek-Oudina, I. L. Animasaun, O. D. Makinde, K. Vajravelu, Hanumesh Vaidya, and D. L. Mahendra. "Unsteady magnetohydrodynamic convective flow of a nanoliquid via a radially stretched rigid area via optimal homotopy analysis method." *Journal of Nanofluids* 11, no. 1 (2022): 84-98. <https://doi.org/10.1166/jon.2022.1818>
- [13] Prasad, K. V., K. Vajravelu, Hanumesh Vaidya, and Robert A. Van Gorder. "MHD flow and heat transfer in a nanofluid over a slender elastic sheet with variable thickness." *Results in physics* 7 (2017): 1462-1474. <https://doi.org/10.1016/j.rinp.2017.03.022>
- [14] Prasad, K. V., Hanumesh Vaidya, Oluwole Daniel Makinde, and B. Srikantha Setty. "MHD mixed convective flow of Casson nanofluid over a slender rotating disk with source/sink and partial slip effects." In *Defect and Diffusion Forum*, vol. 392, pp. 92-122. Trans Tech Publications Ltd, 2019. <https://doi.org/10.4028/www.scientific.net/DDF.392.92>
- [15] Prasad, Kerehalli V., Srikantha B. Setty, Fateh Mebarek-Oudina, Hanumesh Vaidya, Rajashekhar Choudhari, and Isaac Lare Animasaun. "Mixed convective Williamson nanofluid flow over a rotating disk with zero mass flux." *ZAMM-Journal of Applied Mathematics and Mechanics/Zeitschrift für Angewandte Mathematik und Mechanik* 102, no. 11 (2022): e202100117. <https://doi.org/10.1002/zamm.202100117>
- [16] Vaidya, Hanumesh, Rajashekhar Choudhari, Dumitru Baleanu, K. V. Prasad, Shivaleela, M. Ijaz Khan, Kamel Guedri, Mohammed Jameel, and Ahmed M. Galal. "On electro-osmosis in peristaltic blood flow of magnetohydrodynamics

- carreau material with slip and variable material characteristics." *International Journal of Modern Physics B* (2022): 2350032. <https://doi.org/10.1142/S0217979223500327>
- [17] Abbasi, F. M., Maimoona Gul, and S. A. Shehzad. "Effectiveness of temperature-dependent properties of Au, Ag, Fe<sub>3</sub>O<sub>4</sub>, Cu nanoparticles in peristalsis of nanofluids." *International Communications in Heat and Mass Transfer* 116 (2020): 104651. <https://doi.org/10.1016/j.icheatmasstransfer.2020.104651>
- [18] Khashi'ie, Najiyah Safwa, Norihan Md Arifin, and Ioan Pop. "Magnetohydrodynamics (MHD) boundary layer flow of hybrid nanofluid over a moving plate with Joule heating." *Alexandria Engineering Journal* 61, no. 3 (2022): 1938-1945. <https://doi.org/10.1016/j.aej.2021.07.032>
- [19] Bhullar, Malkeet Singh. "Study on properties and applications of Laplace transformation: A review." *Pramana Res. Scholar J* 8, no. 4 (2018).
- [20] Zainal, Nurul Amira, Roslinda Nazar, Kohilavani Naganthran, and Ioan Pop. "MHD flow and heat transfer of hybrid nanofluid over a permeable moving surface in the presence of thermal radiation." *International Journal of Numerical Methods for Heat & Fluid Flow* 31, no. 3 (2021): 858-879. <https://doi.org/10.1108/HFF-03-2020-0126>
- [21] Aladdin, Nur Adilah Liyana, Norfifah Bachok, and I. Pop. "Cu-Al<sub>2</sub>O<sub>3</sub>/water hybrid nanofluid flow over a permeable moving surface in presence of hydromagnetic and suction effects." *Alexandria Engineering Journal* 59, no. 2 (2020): 657-666. <https://doi.org/10.1016/j.aej.2020.01.028>
- [22] Khashi'ie, Najiyah Safwa, Norihan Md Arifin, Ioan Pop, and Roslinda Nazar. "Melting heat transfer in hybrid nanofluid flow along a moving surface." *Journal of Thermal Analysis and Calorimetry* 147, no. 1 (2022): 567-578. <https://doi.org/10.1007/s10973-020-10238-4>
- [23] Roşca, Natalia C., Alin V. Roşca, and Ioan Pop. "Axisymmetric flow of hybrid nanofluid due to a permeable non-linearly stretching/shrinking sheet with radiation effect." *International Journal of Numerical Methods for Heat & Fluid Flow* 31, no. 7 (2021): 2330-2346. <https://doi.org/10.1108/HFF-09-2020-0574>
- [24] Waini, Iskandar, Anuar Ishak, and Ioan Pop. "Hybrid nanofluid flow towards a stagnation point on a stretching/shrinking cylinder." *Scientific Reports* 10, no. 1 (2020): 1-12. <https://doi.org/10.1038/s41598-020-66126-2>
- [25] Farooq, Umer, Muhammad Idrees Afridi, Muhammad Qasim, and DC7513191 Lu. "Transpiration and viscous dissipation effects on entropy generation in hybrid nanofluid flow over a nonlinear radially stretching disk." *Entropy* 20, no. 9 (2018): 668. <https://doi.org/10.3390/e20090668>
- [26] Muthucumaraswamy, R., and T. Kulaivel. "Chemical reaction effects on moving infinite vertical plate with uniform heat flux and variable mass diffusion." *Forschung im Ingenieurwesen* 68, no. 2 (2003): 101-104. <https://doi.org/10.1007/s10010-003-0112-9>
- [27] Muthucumaraswamy, R., and P. Ganesan. "Flow past an impulsively started vertical plate with constant heat flux and mass transfer." *Computer methods in applied mechanics and engineering* 187, no. 1-2 (2000): 79-90. [https://doi.org/10.1016/S0045-7825\(99\)00111-5](https://doi.org/10.1016/S0045-7825(99)00111-5)
- [28] Loganathan, P., and M. Dhivya. "Thermal and mass diffusive studies on a moving cylinder entrenched in a porous medium." *Latin American Applied Research* 48, no. 2 (2018): 119-124. <https://doi.org/10.52292/j.laar.2018.269>
- [29] Parasuraman, Loganathan, and Dhivya Mohanavel. "Numerical investigation on viscous dissipating and chemically reacting fluid over an impulsively started vertical cylinder." *Indian Journal of Pure & Applied Physics (IJPAP)* 56, no. 7 (2018): 551-560.
- [30] Subhashini, S. V., and R. Sumathi. "Dual solutions of a mixed convection flow of nanofluids over a moving vertical plate." *International Journal of Heat and Mass Transfer* 71 (2014): 117-124. <https://doi.org/10.1016/j.ijheatmasstransfer.2013.12.034>
- [31] Loganathan, Parasuraman, and Krishnamurthy Deepa. "Electromagnetic and radiative Casson fluid flow over a permeable vertical Riga-plate." *Journal of Theoretical and Applied Mechanics* 57, no. 4 (2019): 987-998. <https://doi.org/10.15632/jtam-pl/112421>
- [32] Dinarvand, S. A. E. E. D., and M. Nademi Rostami. "Mixed convection of a Cu-Ag/water hybrid nanofluid along a vertical porous cylinder via modified Tiwari-Das model." *Journal of Theoretical and Applied Mechanics* 49, no. 2 (2019): 149-169. <https://doi.org/10.7546/JTAM.49.19.02.05>
- [33] Sulochana, C., and S. R. Aparna. "Unsteady magnetohydrodynamic radiative liquid thin film flow of hybrid nanofluid with thermophoresis and Brownian motion." *Multidiscipline Modeling in Materials and Structures* (2019). <https://doi.org/10.1108/MMMS-08-2019-0160>
- [34] Sadaf, Hina, and Sara I. Abdelsalam. "Adverse effects of a hybrid nanofluid in a wavy non-uniform annulus with convective boundary conditions." *RSC advances* 10, no. 26 (2020): 15035-15043. <https://doi.org/10.1039/D0RA01134G>
- [35] Hassan, Mohsan, Marin Marin, Rahmat Ellahi, and Sultan Z. Alamri. "Exploration of convective heat transfer and flow characteristics synthesis by Cu-Ag/water hybrid-nanofluids." *Heat Transfer Research* 49, no. 18 (2018). <https://doi.org/10.1615/HeatTransRes.2018025569>



- [36] Shit, Sakti Pada, Sudipta Pal, N. K. Ghosh, and Kartik Sau. "Enhanced thermophysical properties of water-based single and hybrid metallic nanofluids: Insights from Equilibrium Molecular Dynamics." *Chemical Thermodynamics and Thermal Analysis* 8 (2022): 100096. <https://doi.org/10.1016/j.ctta.2022.100096>
- [37] Hakeem, A. K., N. Indumathi, B. Ganga, and M. K. Nayak. "Comparison of disparate solid volume fraction ratio of hybrid nanofluids flow over a permeable flat surface with aligned magnetic field and Marangoni convection." *Sci. Iran* (2020). <https://doi.org/10.24200/sci.2020.51681.2312>
- [38] Suneetha, S., K. Subbarayudu, and P. Bala Anki REDDY. "Hybrid nanofluids development and benefits: A comprehensive review." *Journal of Thermal Engineering* 8, no. 3 (2021): 445-455. <https://doi.org/10.18186/thermal.1117455>